Failure of Metallic-Fuel Cladding During Strain Transients

J.C. Rawers, J.A. Buzzell, G.M. Schwartzenberger, G.D. Hudman
EBR-II Project, Argonne National Laboratory, P.O. Box 2528, Idaho Falls, Idaho 83401, U.S.A.

Summary

We have analyzed the conditions of failure stress, failure temperature, and time-to-failure for EBR-II, Mark-II, type 316 annealed stainless steel cladding. The Larson-Miller Parameter (LMP) can be used to predict failure once the irradiation and metallurgical history of the fuel element is given.

Creep failure test and temperature and pressure ramp-to-failure tests have been conducted on type 316 stainless steel fuel cladding. Failure analysis for both sets of test values were summarized in a plot of natural logarithm of effective stress (σ) versus LMP values and showed no differences between results. The LMP versus σ plot for various cladding segments tested could be characterized by two distinct fracture mechanisms. One is independent of irradiation and metallurgical history. The other is highly dependent upon the past metallurgical history (annealed versus cold-worked), and upon the irradiation history (fluence and temperature).

Work Supported by U. S. Department of Energy

1. Introduction

One phase of the qualification program for mild transient cycling of the liquid-metal-cooled Experimental Breeder Reactor No. 2 (EBR-II) is out-of-core failure testing of the type 316 annealed stainless steel fuel cladding. The response to simulated transient conditions of the cladding's material failure temperature, failure stress, failure strain, and time-to-failure were measured in an out-of-core testing device. The cladding was tested to failure under constant pressure and temperature (creep failure) as well as under transient temperature or pressure (transient failure).

The test conditions were set up to simulate at least the most severe expected in-reactor conditions for the cladding. During either steady-state or transient reactor conditions, as the metallic fuel burns up, it swells, contacts the cladding and thereby increases the stress on the cladding. Internal evolution of fission gases also increases the stress on the cladding. Temperature transients cause fuel to expand by transformation of alpha phase to gamma phase which starts at about 550°C. The difference in thermal expansion between the cladding and the fuel also produces a fuel/cladding mechanical interaction during a temperature change. Thus, during a core power cycle (temperature and pressure cycle superimposed upon the normal steady-state reactor conditions), the cladding could experience environmental excursions that might produce sufficient stress to cause cladding fracture.

In the out-of-core studies, described here, the effects of fuel/cladding chemical interactions were not considered.

2. Experimental Procedures

The test apparatus consisted of a laser micrometer, an emissivity-independent optical pyrometer, and pressure transducers, all placed in a hot cell to facilitate testing the radioactive cladding. The laser micrometer could measure changes in diametral strain greater than 0.05%. Diameter measurements were normally recorded ten times per second. The pyrometer used to measure temperature was an analog instrument with a precision better than 2%. The cladding samples were heated by direct element heating. Argon gas was used to pressurize the samples internally. The outputs of the pressure transducers were recorded with an accuracy of $\pm$ 0.3 MPa internal pressure or 2.0 MPa effective cladding stress. All measurements were made without physical contact with the samples. All the instruments, the laser micrometer, the optical pyrometer, and the pressure transducers were checked against standards before and after each test.

The scope of testing included the two extremes in the irradiation conditions for cladding; unirradiated cladding material and irradiated cladding material, which has a nominal fuel burnup of 8 at.% (equivalent to a fluence of $\sim 7 \times 10^{24}$ n/mm^2, E>0.1 MeV). A burnup of 8 at.% is the current limit for EBR-II Mark-II driver fuel. All irradiated cladding was tested from fuel elements of 8 at.% burnup with exception of the mid-fuel cladding segments which were also tested at 1.5, 3.5, 5.5 and 11.5 at.% burnup. The irradiation environment for the fuel element changes along its length in the reactor (see Figure 1). Neutron flux is maximum at the core midplane, but the cladding temperature increases from the fuel bottom ($\sim$370°C) to the fuel top ($\sim$590°C). This change in the irradiation environment can strongly affect the strength and failure properties of the cladding. To understand the effects of the varying irradiation conditions, six 75 mm segments were cut from the cladding of each of the irradiated fuel elements from spent EBR-II driver-fuel subassemblies. The metallic fuel was

chemically dissolved from the cladding.

The creep-failure tests were run at predetermined temperature and pressure values above those normally experienced during steady-state core operations. They were selected to assure failure between 3×10^2 and 3×10^4 seconds. The temperature ramps and pressure ramps of the transient-failure tests were calculated to duplicate the expected ramp conditions that would be observed during a whole-core transient that produces a cladding strain rate of 10^{-5} to 10^{-4} s^{-1}. The expected failure temperature and pressure exceeded any observed steady-state or predicted transient conditions in-core. The temperature and pressure for samples for all tests were first raised to a standard starting condition of 450°C and 60 MPa effective stress.

3. Analysis of Data

Temperature, pressure, and diameter were continuously recorded on a multichannel strip-chart recorder from the standard starting condition settings to failure for all tests. The recorded data were digitized for computer analysis and transformed into corrected temperature, effective stress, and engineering strain as a function of time. Table I lists the various claddings tested (irradiation and fuel segment), the type of test (transient, creep, and ramp rate), the failure values, and calculated failure parameter. The failure stress is reported as effective stress, which was determined from the internal gas pressure and the hoop stress by the von Mises approximation. Recorded temperatures over the testing range of 450-800°C required minor corrections. Calibration and standardization of the emissivity-independent pyrometer were maintained with a black-body source. Strain values were determined from the diameter measurements made by the laser micrometer. They are reported as engineering strains and were calculated based on the cladding diameter at room temperature (d_o). No corrections are made for thermal or elastic expansion. Time-to-failure for the transient-failure tests was measured from the start of the ramp from the standard conditions. Time-to-failure for the creep-failure tests was measured from the moment the test conditions were reached.

The creep and transient results were then analyzed with the intent of establishing failure criteria for the various temperature and pressure irradiation environments of the cladding during whole core transients. The numerous in-reactor irradiation conditions, in addition to the numerous sample variables, forced us to limit the scope of both the testing program and the analysis. The resulting data for failure temperature, failure stress, and time-to-failure were combined using the standard Larson-Miller Parameter (LMP) formulation for creep and the modified LMP formulation for temperature and pressure transients [1].

4. Results

For each segment of a fuel element, a plot of the natural logarithm of effective failure stress versus the Larson-Miller Parameter for temperature and time exhibited two distinct regions (see Figure 2). Preliminary analysis by the scanning electron microscope (SEM) also indicated two different cladding fracture modes, one in each region. The LMP values within each region appear to satisfy a linear relationship. No distinction was observed between the LMP values calculated for the creep-failure tests and the transient tests. The spread in values is well within expected sample-variation and experimental uncertainty.

Each of the two failure regions requires a separate explanation (see Figure 2). In the first region, representing either low temperatures and high ramp rates or high failure

stresses, failure conditions depend strongly on the section of the fuel element tested. Under SEM examination, however, the fracture mode appeared to be the same for all segment failures in this region. The linear relationship for each segment had the same slope but different stress origins. Unirradiated 20% cold-worked segments had a notably higher failure stress than irradiated mid-core segment at the same Larson-Miller value. The mid-core irradiated segments were stronger than other irradiated segments, which were only slightly stronger than the unirradiated cladding. Irradiation hardening of the cladding saturated before a fuel burnup of 3 at.%. The annealing effects of the in-core temperature strongly influenced the resulting failure properties.

In the second failure region, representing either high temperatures and slow ramp rates or low failure stresses, all fuel-element segments (annealed or cold-worked, irradiated or unirradiated, from fuel or plenum regions) appeared to fail by the same fracture mode and along the same line of LMP versus ln σ.

The results from our testing help to increase our capability to predict failure of type 316 stainless steel cladding when the metallurgical and irradiation history of the steel is known.

5. Conclusions

The plots of natural logarithm of effective failure stress versus Larson-Miller Parameter that were prepared from the results of our out-of-core creep-to-failure, temperature ramp-to-failure, and pressure ramp-to-failure testing showed two distinct regions indicating two different failure modes. One, typified by either high failure temperature and low ramp rate or low failure stress is characteristic of the material and is independent of irradiation and metallurgical history. The other mode, typified by either low failure temperature and high ramp rate or high failure stress, is strongly dependent upon past metallurgical history (annealed or cold-worked) and irradiation history (fluence and temperature). Irradiated cladding of annealed type 316 stainless steel has fracture-strength properties intermediate between the unirradiated annealed and 20% cold-worked material. The lower the irradiation temperature and, to a lesser extent, the longer the irradiation temperature, the higher the failure stress becomes, until it approaches the failure stress for the unirradiated 20% cold-worked material.

6. Acknowledgments

The authors gratefully acknowledge the contribution of Dana Berg for review and editing of the paper, and Debbie Reid for preparing the manuscript.

References

[1] STRAALSUND, J. L., FISH, F. L., and JOHNSON, G. D., "Correlation of Transient-test Data with Conventional Mechanical Properties Data," Nuc. Tech., 25, p. 531 (March 1975).

[2] DUNCAN, D. R., "Thermal Creep Effects on 20% Cold-Worked AISI 316 Mechanical Properties," HEDL-TME 80-46 (September 1980).

TABLE I: TRANSIENT AND CREEP CLADDING TEST DATA

Temp °C	σ[a] MPa	ε[b] %	t[c] s	LMP[d]	Ramp[e]	Rate[f]
Unirradiated						
Annealed (U)[g]						
774	271	22.76	105.8	37.31	T	2.83
758	254	10.22	88.6	36.56	T	3.30
593	308	7.46	24	30.44	T	~3
765	281	10.30	288	38.38	T	1
740	283	7.81	85	36.00	T	3
741	281	11.37	31	33.67	T	10.3
542	327	10.93	18.2	29.43	P	13.93
682	261	11.53	13.8	34.29	P	13.49
749	266	12.22	4.6	35.55	P	42.68
765	122	29.1	10040	44.12	Creep	
750	146	16.7	13080	43.76	"	
750	190	26.22	1680	41.65	"	
765	172	35.33	6000	43.57	"	
765	241	22.86	360	40.66	"	
690	213	--	4000	40.00	"	
20% Cold Work (C)						
634	543	1.77	128	33.14	T	1.13
750	394	5.60	255	38.01	P	-
510	576	-	429	30.70	P	-
738	526	-	90	35.3	T/P	-

Temp °C	σ MPa	ε %	t s	LMP	Ramp	Rate
Irradiated 8 at.% Burn-up						
Top Plenum (A)						
547	334	7.5	6.1	28.74	P	52.3
600	324	7.6	47	30.90	T	~3
700	294	7.6	91	34.6	T	2.84
Bottom Plenum (B)						
478	343	8.7	4.1	26.0	P	66.8
758	250	10.0	~39	38.11	Creep	
639	302	5.5	6.3	31.96	P	41.40
737	290	4.5	3.5	34.83	P	60.7
685	284	8.4	106	34.13	T	2.63
Dimple - Interface (I)						
646	312	3.3	2.9	31.5	P	89
700	291	4.6	107.5	34.7	T	~4
Top Fuel (F)						
551	354	2.5	3.7	28.45	P	68
657	310	1.7	3.8	32.13	P	72
755	288	4.0	156	37.54	T	2.6
736	281	2.0	3.3	34.71	P	66
645	327	1.2	3.8	31.71	P	72

Temp °C	σ MPa	ε %	t s	LMP	Ramp	Rate
Irradiated Mid-Fuel						
1.5 at.% Burnup (1)						
577	406	4.62	47.6	30.15	T	2.72
3.5 at.% Burnup (3)						
735	416	4.1	84.9	35.80	T	3.04
775	319	5.0	187.	39.26	T	2.74
5.5 at.% Burn-up (5)						
745	397	1.7	92.4	36.26	T	2.76
546	424	5.0	24.5	29.82	P	13.25
8 at.% Burnup (8)						
741	240	6.1	379	39.38	Creep	
762	322	3.7	156	38.27	T	~3
710	383	2.4	96	35.00	T	~3
11.0 at.% Burn-up (11)						
738	372	1.5	107.4	36.05	T	2.65
557	446	1.1	3.8	28.7	P	111.42

(a) Effective Stress: von Mises Approximation

(b) Engineering Strain: D_o at Room Temperature, Uncorrected for Thermal Exp. or Elastic Stress

(c) Time from Test Condition until Failures

(d) LMP = $T(\ln t_r + 33)$; $T(^oK)$, $t_r(s)$

(e) T = Temperature, P = Pressure

(f) For Temperature Ramp: $^oCS^{-1}$, For Pressure Ramp: $MPaS^{-1}$

(g) Notation used in Figure 2

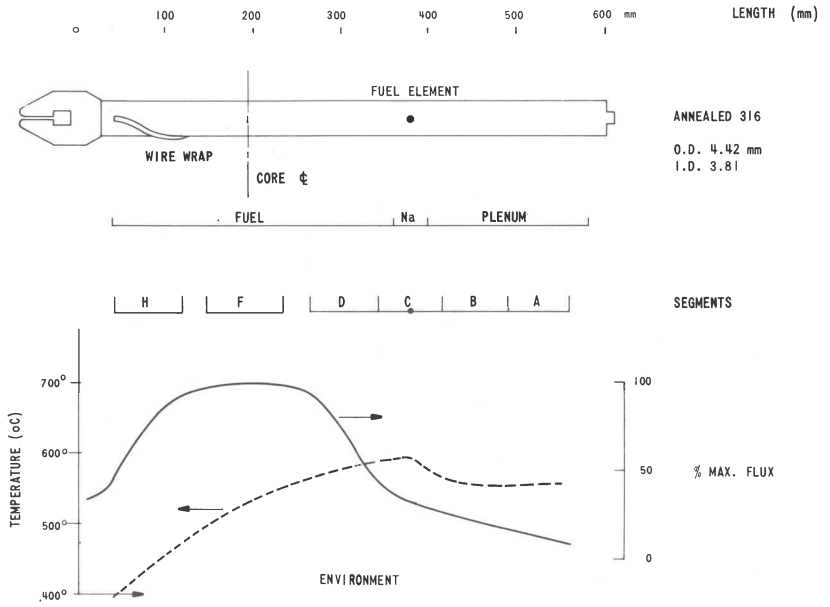

Figure 1. Fuel Pin, Segments, Dimensions, Thermal and Fluence Environment.

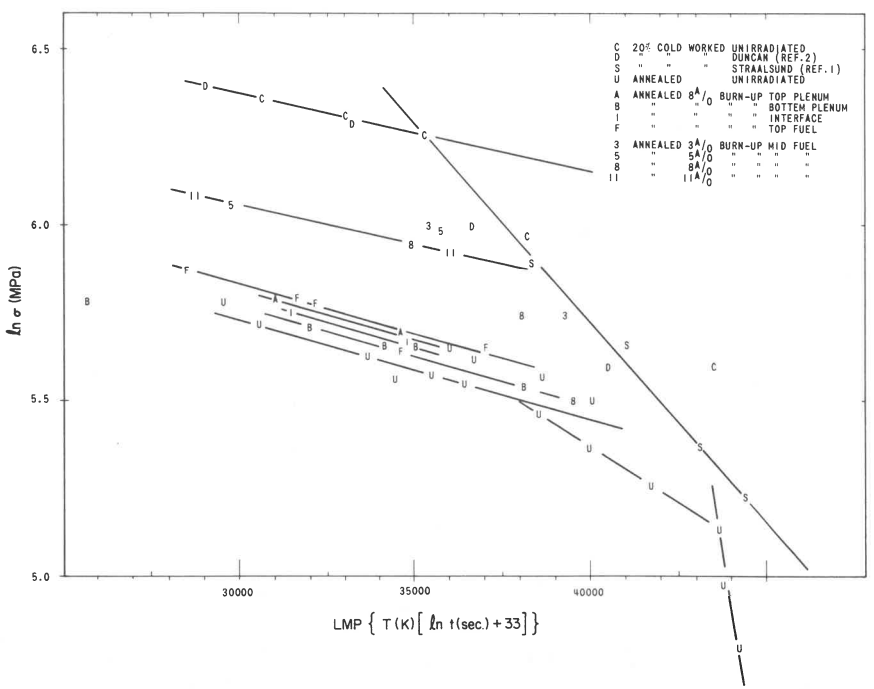

Figure 2. Larson-Miller Parameter versus Effective Fracture Stress.